Geothermics 50 (2014) 1–9

Contents lists available at ScienceDirect

Geothermics

journal homepage: www.elsevier.com/locate/geothermics

Types of the scaling in hyper saline geothermal system in northwest Turkey

Mustafa M. Demir[a], Alper Baba[b,*], Vedat Atilla[c], Mustafa İnanlı[c]

[a] Izmir Institute of Technology, Department of Chemistry, 35430 Gülbahçe, Urla, İzmir, Turkey
[b] Izmir Institute of Technology, Geothermal Energy Research and Application Center, 35430 Gülbahçe, Urla, İzmir, Turkey
[c] ENDA Energy, 35220 İzmir, Turkey

ARTICLE INFO

Article history:
Received 13 February 2012
Accepted 1 August 2013

Keywords:
Tuzla
Geothermal fluid
Scaling
Hydrogeochemistry
Lead

ABSTRACT

Tuzla is an active geothermal area located in northwestern Turkey, 80 km south of the city of Canakkale and 5 km from the Aegean Coast. The geothermal brine from this area, which is dominated by NaCl, has a typical temperature of 173 °C. Rapid withdrawal of fluid to ambient surface conditions during sampling causes precipitation of various compounds known as scaling. Scaling is one of the important problems in Tuzla geothermal system that reduces the efficiency of the geothermal power plant and causes economical loss. The aim of this study was to determine the type of scaling as a first step towards preventing its formation. The scales formed in the geothermal system were divided into two groups according to location: the ones that formed in downhole and the ones that accumulated along the surface pipeline. Both scales were examined in terms of their elemental composition, structure and morphology using XRF, XRD, and SEM, respectively. The former was found to be mainly composed of PbS (Galena) and $CaCO_3$ (aragonite or calcite). In contrast, the latter was heterogeneous in nature and consisted of mainly saponite like amorphous structure along with submicrometer-sized amorphous silica particles, layered double magnesium and iron hydroxide, and NaCl.

1. Introduction

Geothermal fluids are saturated with silica and are typically close to saturation with calcite, calcium sulphate, calcium fluoride, magnesium silicate, aluminium-silicates, opaline silica, iron–magnesium-silicates, and metal sulfide (Gunnlaugsson, 1989; Kristmannsdóttir, 1989; Honegger et al., 1989; Ölçenoğlu, 1986; Patzay et al., 2003). The reduction of temperature and pressure during production lowers the solubility and causes prodigious precipitation known as scaling. Literally tens of different types of scales have been reported. Depending upon the reservoir temperature and the chosen brine production and utilization processes, four major types of scale are encountered: (1) Carbonates such as calcium and strontium carbonates. (2) Silica and other siliceous materials. (3) Heavy metal sulfides. (4) Various types of exotic chlorides. However, calcite and silica deposits are the most frequent scale formation materials. Scale formation is a common problem in many geothermal energy exploitations (Juranek et al., 1987; Arnorsson, 1989; Gill, 1998; Potapov et al., 2001; Gallup, 2002). The most troublesome scaling deposits usually occur in the well casing at the level of first boiling (bubble point) (Patzay et al., 2003). They can be defined as hard adherent mineral deposits that precipitate from brines. The amount and location of scale depend on different factors, such as the degree of supersaturation, kinetics, solution pH and composition, CO_2 content, temperature, and pressure (Garcia et al., 2005). The most extreme cases are due to precipitation of calcium carbonate in brackish water and occur both in downhole pumps and surface installations. Silica scaling in waste water is a general problem in most sites (Kristmannsdóttir, 1989). Scaling in several Turkish wells caused scale of 3 cm thickness, leading to a 50% reduction in cross-section without flow problems at the wellhead (Ölçenoğlu, 1986; Şimşek et al., 2005). Well production and injection capacities undergo serious decline due to scaling therefore resulting serious damage to utilization systems and consequent economic loss. Scale prevention is, therefore, the most important action that must be taken at the sites. Accordingly, the chemical identification and description of the scale formed during production are of primary importance.

Geothermal fluids have been utilized for energy production in Tuzla geothermal field (TGF), which is located in northwestern Turkey, 80 km south of the city of Canakkale and 5 km from the Aegean Sea (Fig. 1). An Organic Rankine Cycle (ORC) binary plant has been selected and constructed by Ormat Company. The two phase geothermal fluid coming from the production wells is segregated at wellhead separators to steam and brine. While steam flows to the power plant naturally, brine is pumped to the power plant by

* Corresponding author. Tel.: +90 232 750 68 07; fax: +90 232 750 68 01.
E-mail address: alperbaba@iyte.edu.tr (A. Baba).

0375-6505/$ – see front matter © 2013 Elsevier Ltd. All rights reserved.
http://dx.doi.org/10.1016/j.geothermics.2013.08.003

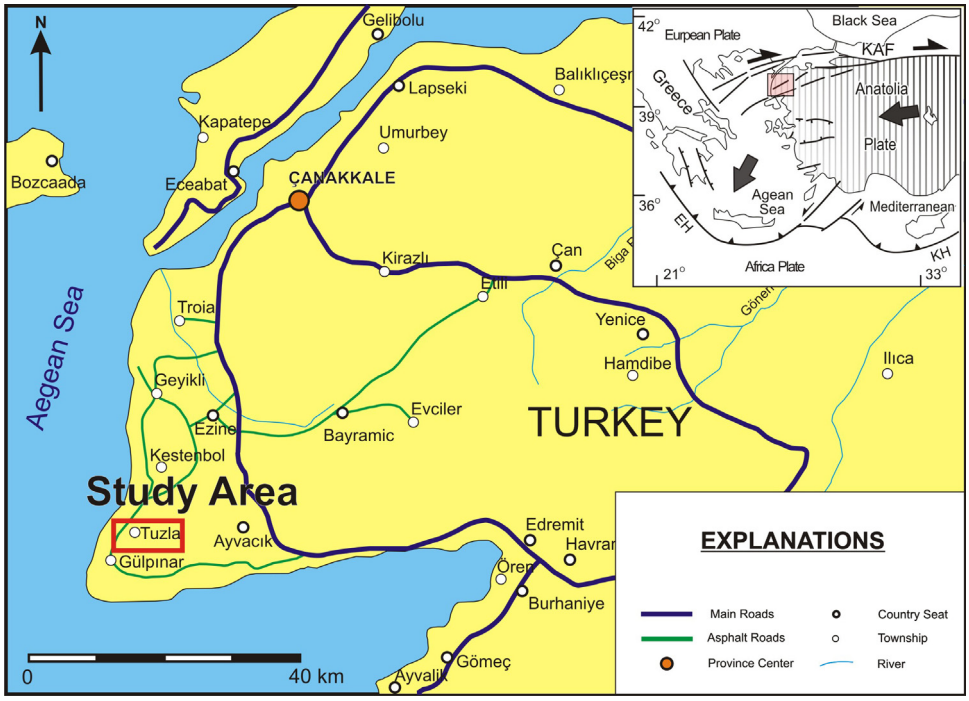

Fig. 1. Tuzla geothermal field.

booster pumps. Steam and brine transfer their thermal energy to *n*-pentane that is circulating in the electromechanical equipment in the plant, while passing through heat exchangers called vaporizers and preheaters. Later, the geothermal fluid is re-injected back into the reservoir. Two reservoir wells (T9E and T16E) have been used to produce fluid (Fig. 2). The wellhead pressure of T9E and T16E is 3.6 bar and 3.72 bar, respectively. These wells are artesian flow. No pumps have been used in these wells.

In the Tuzla geothermal system, silicate-based scaling, which is the most difficult scaling to remove, is readily observed. Therefore,

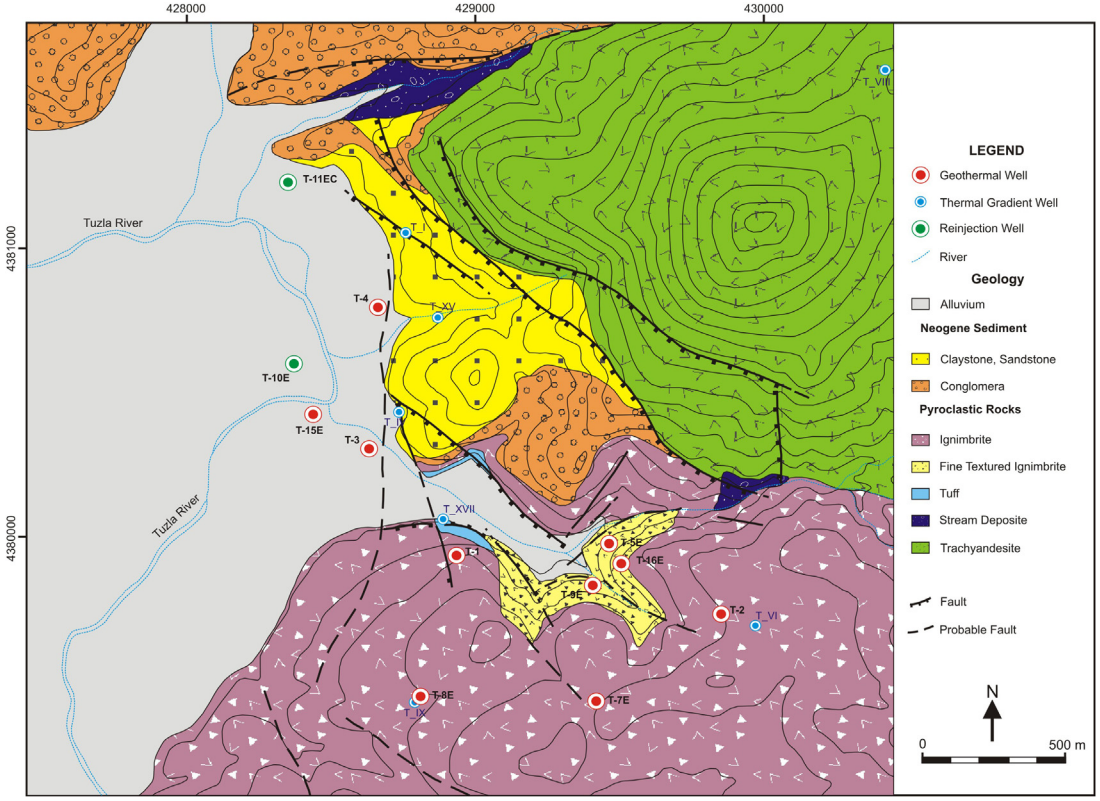

Fig. 2. Geological map of study area.

Modified from WES JEC (2006) and HU (2008a,b).

in this work, the focus was on detailed examination of this scale. The results of this examination yield valuable information on the formation mechanism of the scale that may improve our understanding of the causes of the scaling.

2. Geological and hydrogeological properties of study area

Tuzla is an active geothermal area hosted by rhyolite lava and pyroclastic deposits. Geothermal brine is found in a shallow volcanic reservoir at a depth of between 330 m and 550 m and a deep marble reservoir has been detected at depth of 530 m. Tuzla geothermal field is an interesting area in Turkey because of its temperature and dissolved ions in the water. The chloride concentration of Tuzla geothermal brine reaches 36,380 mg/L, which is nearly twice the concentration of seawater and is termed "brine" water. Furthermore, the sodium concentration reaches up to 19,350 mg/L.

Geothermal studies on the Tuzla geothermal field (TGF) have been ongoing since 1966. The general geological, geophysical, hydrogeological and environmental characteristics have been studied by Şamilgil (1966), Erdogan (1966), Ürgun (1971), Öngür (1973), Alpan (1975), Demirörer (1971), Ekingen (1972), Karamanderesi and Öngur (1974), Gevrek and Sener (1985), General Directorate of Mineral Research and Exploration (MTA) (1997), Şamilgil (1983), Şener and Gevrek (2000), Baba and Özcan (2004), Baba (2003), and Baba et al. (2005, 2009). Ten deep exploration wells (with a depth range of 539–1020 m) were drilled from 1982 to 2008 by MTA and Tuzla Jeotermal A.Ş. Two reservoir rock types (volcanic and metamorphic) have been determined in the study area. The reservoir depths are in the range of 330–550 m in volcanic rock and over 530 m in metamorphic marbles with a temperature of 173 °C. Hydrothermal alteration mineral assemblages indicate a geothermal fluid with temperatures of 150–220 °C (Şener and Gevrek, 2000). Similarly, Mutlu and Güleç (1998) calculated the reservoir temperature of Tuzla to be between 187 °C and 212 °C using different geothermometers. Solute geothermometry techniques were applied to hot waters from springs in Tuzla geothermal by Baba and Deniz (2005). The results of this study show that geothermometer applications indicate subsurface reservoir temperatures that range from 182 °C to 232 °C. According to isotope data, Tuzla geothermal fluid comes from connate water in the Tuzla area (Mützenberg, 1997; Baba et al., 2009).

Metamorphic rocks (marble and schist) and granite intrusion have been recovered from drill cores, but do not crop out at the surface. Metamorphic rocks are seen in some drill cores (T10E) (see Fig. 2) at 525 m and a granitic intrusion is seen at 778 m (T11E) depth in the plain area. The basement rocks are overlain by Tertiary strata comprised of pyroclastic rocks, rhyolite tuff, sedimentary units (gravel, sandstone, claystone and marl) and rhyodacite lava (Fig. 2). These tertiary strata are highly altered and covered by Quaternary sediments and alluvium. The currently active thermal regime is associated with volcanism. Generally, the major geologic structures in the TGF are recognized to be N–S and NW–SE trending fault systems (Fig. 2). The N–S trending fault system is situated at the boundary of Neogene sediments and Quaternary alluvium. Along the N–S trending fault system, many geothermal springs are developed. The major faults trending NW–SE along the western and southern slope of the Tuzla Tepe are normal faults.

3. Method

3.1. Water and scale sampling

Six geothermal water samples, including two from geothermal production wells, two from the well separators and two from inlet and outlet vaporizers, were collected in Tuzla geothermal field. The locations of the production wells, where water samples were collected, are shown in Fig. 2. The collection of samples from high-temperature fluid was achieved by using the separator. One-litre glass bottles were used for major ions and for trace metal analyses in the water. When sampling, all water samples were filtered through 0.45 μm membranes on site. Unstable hydrochemical parameters including electrical conductivity (EC), temperature (°C) and pH values were measured in situ with a multiparameter instrument that had been calibrated before use. Alkalinity was measured using the titration method. The concentrations of SO_4^{2-}, Cl^-, Ca^{2+}, Mg^{2+}, Na^+, and K^+ were determined by ion chromatography, SiO_2 by colorimetry and other chemical constituents (B, Ba, Cr, Fe, Li, Pb and Zn) by ICP-MS within one week after sampling (Table 1).

The scaling samples were obtained from different places in the system. The well scales were collected from the surface of the inhibitor hose at different depths: 15-30-45-60-75 m. The samples in the pipeline were taken from the ORC brine inlet filters, the brine inlet valve, the pipeline between well T9E and T16E, the wellhead booster pump outlet and the wellhead.

3.2. Characterization tools

Density of the scale was estimated by dividing mass (measured by gravimetry) to volume (determined by the displacement of water). The morphology of the scale at macro and micro levels were obtained by microscopy. Optical microscopy (Olympus BX51, Essex) was used to image the crossection of the scales. Scanning electron microscopy (FEI Philips XL30 sFEG, Oregon) coupled with energy dispersive X-ray spectrometry (EDX) was carried out using SE and BSE detectors to determine surface features and local chemical contents. The samples were used as they were, without any coating. The crystal structure of the synthesized particles was characterized by X-ray diffraction (XRD, Philips X'pert Pro, Almelo) with a Cu Kα radiation source (λ = 1.54 Å). The average size of crystallites was determined by Scherrer's equation

$$t = \frac{0.9\lambda}{B\ \cos\theta} \quad (1)$$

where t is the size of the particle, λ is the wavelength of Cu Kα radiation and B is the line broadening. X-ray fluorescence (XRF, METEC spectro IQ II, Kleve) analyses were performed on scale powder for the determination of elemental composition. X-ray source was operated at 50 kV and 25 mA with a tantalum disc collimator. The detector was an Amptek XR-100CR with detection area size of 7 mm^2, silicon thickness of 300 mm, and Be window of 12.5 mm. The X-ray source and the detector were placed at 90° with respect to each other.

4. Hydrogeochemical properties of geothermal brine

In geothermal water samples from Tuzla, the average pH and EC values range from 6.14 to 7.74 and from 90.6 to 93.2 mS/cm, respectively. The pH value in the system is changing continuously. The water from the wells is acidic due to an excess of free CO_2 (free mineral acidity) which is the result of the high partial pressure of this gas in the well. The temperature of geothermal fluid in well T9E and T16E in Tuzla geothermal site is 149.1 °C and 150.6 respectively (Table 1). The wellhead pressure ranges from 3.61 to 3.74 bar in production wells. The pressure after separator of these wells ranges from 3.61 to 3.74 bar. The vaporizer inlet brine pressure ranges from 3.1 to 3.5 bar.

Sodium and chloride are the dominant ions in the geothermal brine of the Tuzla region. According to the Piper and Schoeller diagrams in Fig. 3a and b, the geothermal brine are in NaCl facies (in the same facies as seawater) in annual periods (both dry and wet

Table 1
Chemical composition of geothermal fluids (nd: no data).

Sample no.	Sample location	pH	EC (mS/cm)	T (°C)	P (bar)	Na (mg/L)	K (mg/L)	Mg (mg/L)	Ca (mg/L)	Cl (mg/L)	SO_4 (mg/L)	HCO_3 (mg/L)	SiO_2 (mg/L)
T1	T16E well	6.2	91.4	150.6	3.74	18,970	1.81	107	2.95	34,280	167	140	196
T2	T16E Separator	7.6	91.9	142.5	6.18	19,170	1.87	102	2.96	34,150	165	133	204
T3	T9E well	6.14	90.6	149.1	3.61	19,320	1.90	115	3.02	34,740	16	118	195
T4	T9E Separator	7.74	93.2	142	4.97	19,350	1.89	111	2.99	36,380	181	117	189
T5	Vaporizer Inlet Brine	7.65	91.9	142	3.1–3.5	19,330	1.93	119	3.05	35,960	183	115	225
T6	Vaporizer Output Brine	nd	nd	123.4	2.2	19,280	1.87	87	3.00	35,320	190	116	nd

Sample no.	B (mg/L)	Ba (mg/L)	Cr (mg/L)	Fe (mg/L)	Li (mg/L)	Pb (mg/L)	Zn (mg/L)	Sr (mg/L)
T1	75.1	5.9	3.2	5.08	25.6	<40	0.65	175.8
T2	64.2	5.0	1.9	5.68	22.4	5.9	0.35	148.2
T3	60.5	5.1	1.2	6.20	21.6	<40	<0.30	145.5
T4	55.5	5.1	0.5	5.96	21.2	<40	0.46	142.4
T5	50.2	5.0	2.5	4.25	19.9	<40	<0.30	131.7
T6	53.8	6.0	0.8	nd	23.5	<40	<0.30	153.8

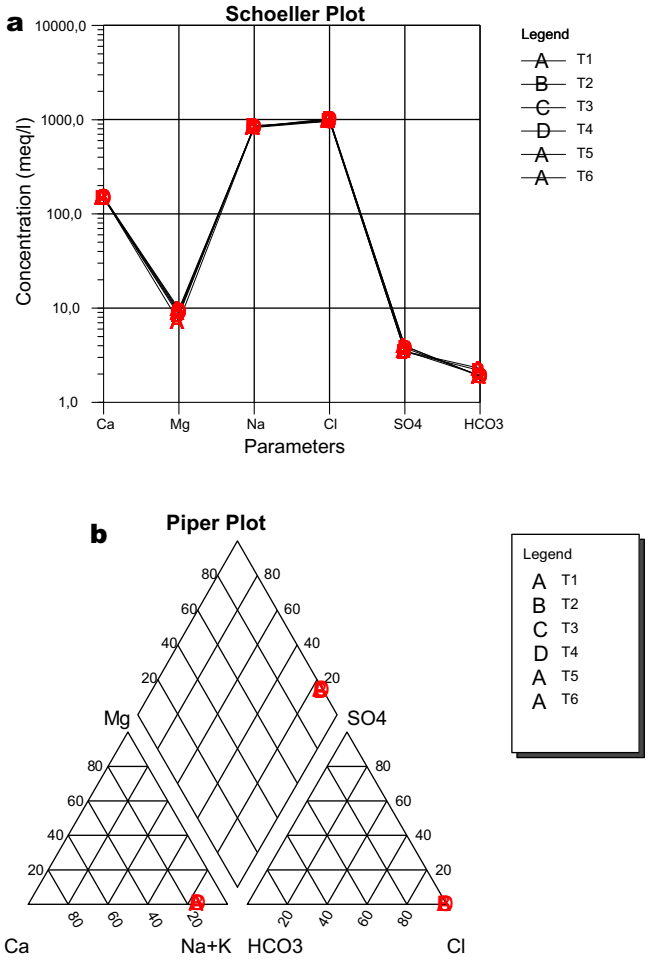

Fig. 3. Chemical analysis of water of the study is plotted on (a) Schoeller and (b) Piper diagram.

periods). The emergence of geothermal brine can be as a result of extensional tectonic regime where lithosphere is thinner and uplift occurs due to isostasy (Keisuke, 1978). Active seismicity in the region makes it easier for liquid to ascend at depth. The ascending brine is to some extent cooled and diluted by mixing with groundwater. The outflowing of NaCl rich thermal brine indicates the presence of hydrothermal activity (Mützenberg, 1997; Baba et al., 2009).

The black and reddish colour of geothermal brine with high Mg and Fe content is attributed to the dissolution of ferromangnesium minerals within Miocene volcanic rocks which consist of trachyte, andesite, and trachyte andesite. Highly altered, these rocks include quartz, K-feldspar, biotite, amphibole, sanidine, chalcopyrite, pyrite and hematite (Karamanderesi and Öngür, 1974). The high trace metal content in the hot-saline waters of the TGF results from rapid evolution of anoxic conditions in brines (Drever, 1997) and reduction of the sulphite (SO_3) formed by reactions with trace elements, followed by release of trace elements during oxidation of the metal sulfides by bacterial activities. Some metals were analyzed in geothermal fluid in Tuzla (see Table 1). The concentrations of these minor components B, Ba, Cr, Li, Zn and Sr range from 50.2 to 75.1; from 5.0 to 6.0; from 0.5 to 3.2; from 19.9 to 25.6; from <0.30 to 0.65; and from 131.7 to 175.8 mg/L, respectively of the geothermal waters. B and Sr concentrations in geothermal fluids are extremely high in the Tuzla geothermal field. This is related to volcanic rocks but may also be controlled by the degassing of magma intrusives. Of these trace metals, Zn and Pb are known to build stable chloride

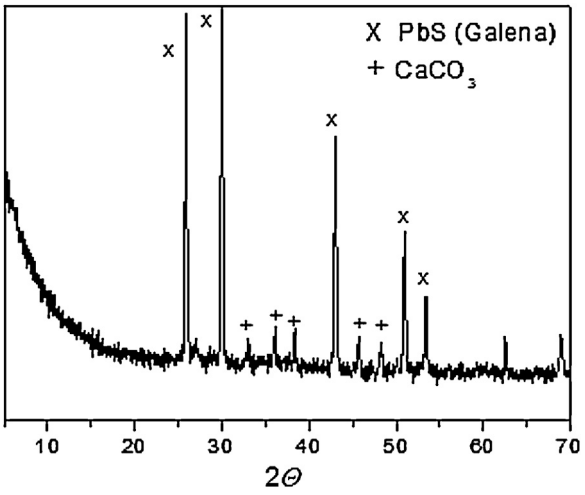

Fig. 4. XRD pattern of a representative well scale.

complexes at high temperatures (White, 1968). Also, Tuzla brine includes silica (SiO_2) (195–225 mg/L). Quartz is soluble in the brine in the reservoir under high pressure and high temperature (Newton and Manning, 2000). Silicic acid – H_4SiO_4 or more properly $Si(OH)_4$ – is the chemical form of silica dissolved in water. The concentration of silicic acid, which is in fact the concentration of silica, in geothermal brine is in nearly all cases determined by the solubility of quartz in the reservoir, and depends primarily on temperature, secondly on salt concentration, and lastly on pH. The equilibrium controlling the silica concentration is:

$$SiO_2(Qtz) + 2H_2O \rightarrow Si(OH)_4(aq)$$

Flashing (a rapid decrease in pressure and temperature) the brine does not produce silicic acid which is in any case a very weak acid. At some point if the brine flashes in the well then the pH of the brine increases while CO_2 separates from brine. The reaction to form metal silicates requires an hydroxide ion, therefore, it takes place only after steam is separated from the brine, increasing pH and the concentration of $[OH]^-$ in the brine.

$$3Mg^{2+} + 4Si(OH)_4 + 6OH \rightarrow Mg_3Si_4O_{10}(OH)_2 + 10H_2O$$

In the reservoir and in the well bore prior to steam separation, the concentrations of Mg and Fe in the brine are at equilibrium with Mg and Fe minerals in the reservoir rock at the pH that exists in the reservoir and in the absence of precipitation. The high NaCl content of the Tuzla brine accelerates the scaling reaction of Mg and Fe.

5. Result and discussion

5.1. Identification of the scales

The scales obtained from the entire system were divided into two groups with respect to the place they formed: scales in the downhole and scale in the surface pipeline. Their examination in terms of structure, elemental composition, and morphology is given in the following sections.

5.1.1. Scales in downholes

In the downhole, inhibitor of $CaCO_3$ encoded with GE WATER PDC 9332 was applied to 180 m depth with a dosage of 3 ppm. However, scaling was observed on the surface of the inhibitor hose. It was mainly composed of lead, iron, silicon, calcium, and traces of other elements. The scale was black and its density was between 2.18 and 2.88 g cm^{-3} depending on the metal content in the scale. Fig. 4 presents a representative XRD pattern of the scale obtained in the well. The sharp reflections suggest that the deposit contains a highly crystalline structure. A number of reflections with high intensity designated with × were well indexed with PbS (galena, Reference code: 00-005-0592). The crystallite size of PbS was found to be 60 nm according to the application of the Debye–Scherrer equation to the most intense signal of cubic PbS crystal, (1 1 1). The rest of the reflections were characteristic signals of $CaCO_3$ marked with + in the diffractogram. However, the crystal structure of $CaCO_3$ varies depending on the depth of the scale samples provided. From the surface to a depth of 30 m in the well, $CaCO_3$ precipitates as calcite form. Below this depth, the formation of aragonite was observed. The mineralogical difference between calcite and aragonite deposits is clearly reflected by the difference of thermodynamic conditions. Aragonite is thermodynamically unstable at ambient conditions but it has stability at elevated temperatures and pressures (MacDonald, 1956). This is because the precipitation of $CaCO_3$ turns from calcite to aragonite as the temperature and pressure increase through the well.

The top panel of Fig. 5 illustrates the optical microscopy image of the crosssection of the scales in the well. The structure is composed of layers with different thicknesses on the order of millimetres. The layers appear as black and white colour that are likely due to the PbS and $CaCO_3$, respectively. They were respectively designated with letters of a and b. A SEM equipped with EDX is very effective for the characterization of the scales because each layer can be separately characterized. The results of EDX are complimentary to the information provided by XRD. EDX spectrum taken from the zone a is rich in terms of Ca and O. The signals of $CaCO_3$ in XRD are compatible with this result. On the other hand, zone b mostly contains Pb and S. Both elements appear at the same energy level in the EDX spectrum so their signals interfere with each other. A clear spectrum to resolve this interference, wavelength dispersive spectroscopy attached to SEM, would be beneficial for further studies. Nevertheless, the results are compatible with the results given in the XRD (Fig. 4). Note that the white and black colours differ in photographic and microscopic images. The white colour in the photo refers to a $CaCO_3$ region; on the other hand, the black colour corresponds to the heavy metal atoms in the backscattered electron microscopy image. Similarly, the black colour in the SEM image represents PbS whereas the white colour refers to the $CaCO_3$ matrix.

The scales collected from different depths were subjected to elemental analysis using XRF. The thickness of the scale was around 7 mm, which forms in 4 months. Bulk chemical compositions of all the scales measured by XRF were collected and evaluated with respect to the depth in the downhole. Fig. 6 shows the elemental composition of the scales obtained by XRD in terms of Pb, Fe, Ca, Si, and Mg. The appearance/disappearance of elements corresponds to changes in depth of the recovered scale. Galena was found in the scales obtained from all depths. As the depth decreases, i.e. through the wellhead, the concentration of Pb in the scale decreases dramatically indicating that the reservoir is rich in terms of Pb. In contrast, the content Fe in the scale increases with decreasing depth. This result suggests that the precipitation of Fe-based compound occurs in the 75–15 m depth. The concentration of Ca in the deposit varies as a function of depth. The fluctuation of the concentration of these elements might be due to application of the inhibitor used to reduce formation of $CaCO_3$. The concentration of SiO_2 decreases with depth down to 60 m (from ca 22 to 14 wt%) then show a linear increase through the surface. In contrast, Mg remained almost unchanged with respect to depth. A detailed composition of a representative scale obtained from a depth of 30 m is given in Table 2. It is found that the composition of this representative scale can be considered as a reflection of the elemental composition of water. The deposit is mainly composed of Fe, Ca, Si, Mg, and P. It is worthy to note that the amount of Sr is unexpectedly higher in the structure of the deposit, which is

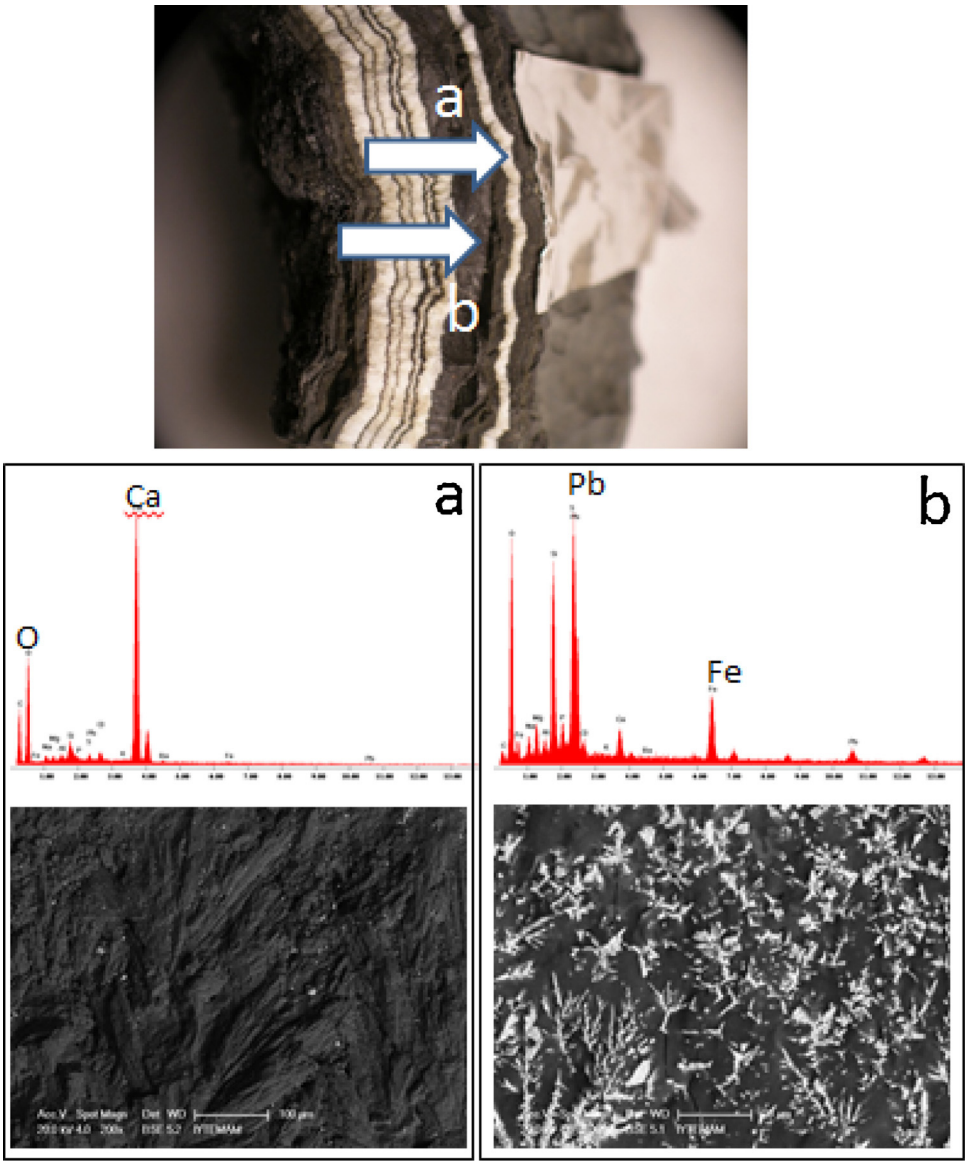

Fig. 5. Photographic image of crosssection of scale. Layer-by-layer structure is evident. (a) EDS spectra of the layer a shown by arrow a and (b) EDS spectra of the layer b shown by arrow b.

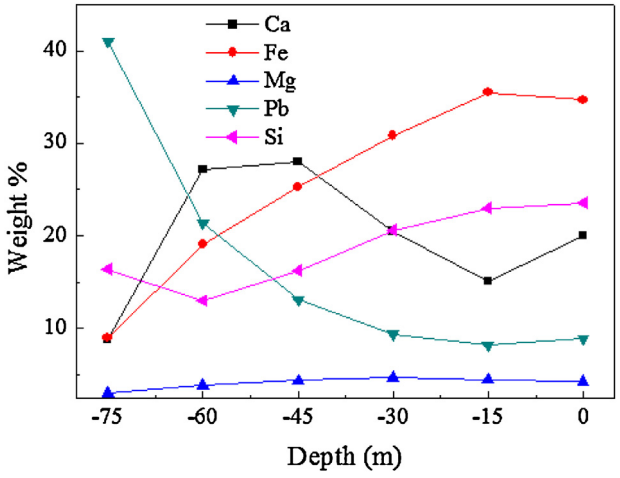

Fig. 6. Elemental composition of scales in the well obtained by XRF as a function of height the scale collected. The samples are collected from the surface of inhibitor hose.

rare in the geothermal fields of Turkey. In addition to the elements listed above, Mn and Al were detected most probably coming from the altered volcanic rocks which are crop out around study area.

5.1.2. *Scales in surface pipeline*

The scale of the pipeline also appeared black and its density is $2.183 \pm 0.003\ g\ cm^{-3}$. The scale was heterogeneous in nature and was a mixture of various components. The samples were collected from seven different places within the system. All of the scales exhibited similar structure in terms of composition and morphology. Inhibitor containing GE WATER GN7004 was applied to the system with a dosage of 6 ppm. Fig. 7 illustrates the XRD pattern of the scale. Diffraction signals at $2\theta = 19.6^{\circ}$, 34.7°, and 60.8° were observed and assigned to saponite. The signals are broad and of asymmetric shape with tails elongating to the higher 2θ indicating that the structure of the material is disordered. This pattern may be attributed to a complex clay mineral known as iron and magnesium silicate, a typical formula is $(Mg,Fe)_2Si_5O_{13}(OH)_2$. In the case of a crystal, there is order in the arrangement of atoms. On the other hand, in the geothermal plants, brine is pulled out by

Table 2
XRF bulk composition of a representative scale obtained from depth of 30 m.

Atomic number (Z)	Element	Concentration (%)	Abs. error (%)	Atomic number (Z)	Element	Concentration (%)	Abs. error (%)
11	Na	0.889	0.057	37	Rb	<0.00030	(0.0)
13	Al	0.8899	0.0076	38	Sr	0.2912	0.0020
14	Si	9.889	0.020	39	Y	<0.00071	(0.0)
12	Mg	2.247	0.024	40	Zr	<0.051	(0.0)
15	P	1.496	0.005	41	Nb	0.00381	0.00037
16	S	0.4096	0.0028	42	Mo	0.00161	0.00043
26	Fe	14.81	0.03	47	Ag	0.02043	0.00064
20	Ca	9.831	0.029	48	Cd	0.00615	0.00055
22	Ti	<0.00051	(0.0)	49	In	<0.00051	(0.0)
25	Mn	0.8928	0.0097	50	Sn	<0.00061	(0.0)
19	K	0.1419	0.0069	51	Sb	<0.00061	(0.0)
24	Cr	<0.00051	(0.0)	52	Te	<0.00071	(0.0)
17	Cl	0.3524	0.0012	53	I	0.0040	0.0021
23	V	0.0301	0.0029	55	Cs	0.00091	0.00091
27	Co	<0.00030	(0.0)	56	Ba	0.678	0.013
28	Ni	<0.00020	(0.0)	57	La	<0.0010	(0.0)
29	Cu	0.0074	0.0030	58	Ce	<0.0012	(0.0)
30	Zn	0.0641	0.0020	72	Hf	<0.00020	(0.0)
31	Ga	<0.00010	(0.0)	73	Ta	0.2721	0.0083
32	Ge	<0.00010	(0.0)	74	W	<0.00020	(0.0)
33	As	<0.00010	(0.0)	78	Pt	0.00001	0.00001
34	Se	<0.00010	(0.0)	79	Au	0.00001	0.00001
35	Br	0.00078	0.00069	80	Hg	<0.00020	(0.0)

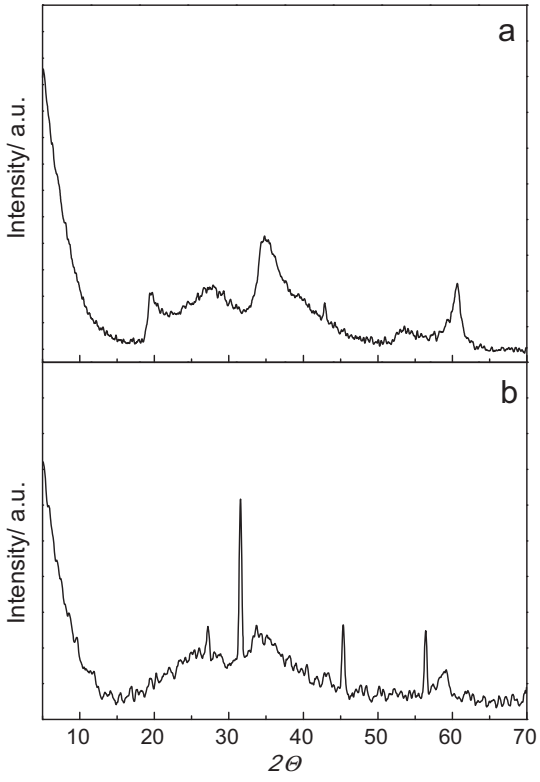

Fig. 7. XRD of representative scales obtained from (a) pipeline (saponite/hectorite). (b) Pump output (NaCl).

pumps suddenly. Therefore, atoms do not have enough time to orient themselves in a perfect order as occurs in nature. The scaling in the pipeline thus appears to be an amorphous structure.

The morphology of the scales was examined by SEM (Fig. 8). Two different morphologies were found in almost all scale samples. One of them can be seen in Panel a of Fig. 8. Submicron sized platelet-like flakes that were randomly placed without any preferential orientation were present. This morphology is unique for double layered hydroxides (LDHs). LDH is a class of lamellar solids with positively charged layers with two kinds of metallic cations (iron and magnesium in our particular case) and exchangeable hydrated anions for example CO_3^{2-} and PO_4^{3-} (Demir et al., 2006; Meyn et al., 1990). They are commonly represented by the formula $[M_{z+1-x}M_{3+x}(OH)_2]^{q+}(Xn\text{-})q/n{\cdot}yH_2O$. However, this structure was not decisive for identification by our X-ray diffractograms due to both their amorphous structure and their low abundance in the scale. Another common morphology in the structure of scales of surface pipeline can be seen in Panel b of Fig. 8. It shows spherical colloids whose size is 1.3 ± 0.6 μm. The particles merge during contact to form an accretion (coalescence). This morphology is quite similar to amorphous silica particles that have been reported previously many times in literature (Lin et al., 2011; Pol et al., 2003).

The mechanisms of scaling have been studied in detail in literature; however, understanding the formation of silicate scaling has not yet been fully developed. There are many proposed mechanisms. One of the most accepted hypotheses on scale formation is based on the reaction between amorphous silica and metal hydroxides formed as a result of increased pH (Demadis, 2010). According to this hypothesis, the occurrence of both scaling components described above is induced by the separation of CO_2 from the geothermal fluid. CO_2 is initially soluble in the reservoir. It is in fact an acidic gas and originates from a weak acid, H_2CO_3. When this gas is evaporated near flashing point in the downhole, the solubility of CO_2 in the brine decreases and the removal of CO_2 causes an increase of pH. The medium appears to be basic and catalyzes the formation of water insoluble metal hydroxides ($Mg(OH)_2$ and $Fe(OH)_2$) as well as layered double hydroxides. Simultaneously, the basic medium directs the polymerization of silicic acid that has four OH groups (Buckley and Greenblatt, 1994). The condensation of intermolecular reactive OH groups forms bridging oxygen or a siloxane groups Si—O—Si. A water molecule is eliminated. This polycondensation reaction occurs at numerous sites. When sufficient number of Si—O—Si groups form, they nucleate and grow into colloidal particles. The mechanism is outlined in detail below.

$$(HO)_3Si(OH) + HO^- \leftrightarrow (HO)_3Si\text{-}O^- + H_2O$$

$$(HO)_3Si\text{-}O^- + (HO)Si(OH)_3 \leftrightarrow (HO)_3Si\text{-}O\text{-}Si(OH)_3 + HO^-$$

The scales observed along the surface pipeline are a result of the reaction between metal hydroxides and colloidal silica.

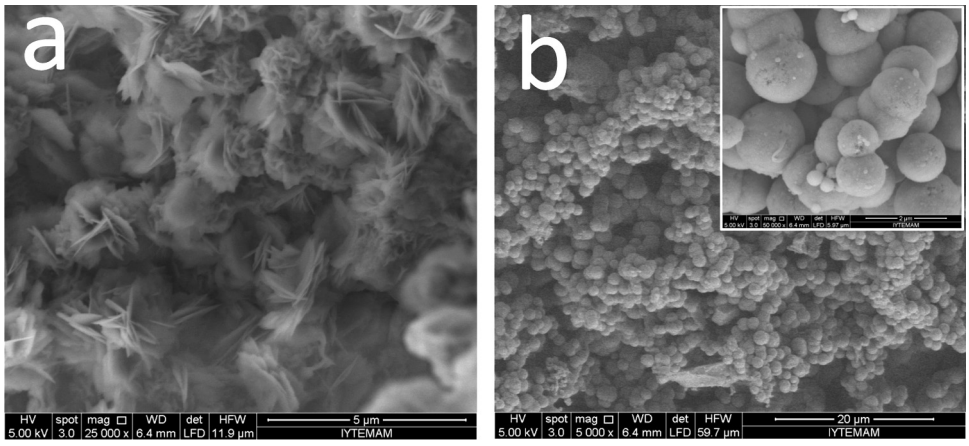

Fig. 8. SEM images of the scale in the pipeline indicating the presence of (a) amorphous silica and (b) layered hydroxide.

6. Conclusion

The scales observed in Tuzla geothermal system were examined in detail according to location: scales in the down hole or scales in the surface pipeline. PbS and $CaCO_3$ were detected in the downhole and the surface pipeline. In contrast, sulfide based-scaling was encountered only in the downhole, not along the surface pipeline. In addition, the following chemical species were identified in the scale obtained from the pipeline: saponite like amorphous structure as main component, layered double hydroxide, and NaCl. A systematic study to develop new methods/inhibitor molecules for the minimization of the scale formation in Tuzla is underway.

Acknowledgements

The authors acknowledge The Centers of Materials Research and Environmental Research of at Izmir Inst. Technol. for assistance in all measurements. The authors are grateful to Dr. J. Icenhower and Ms. Marilyn Smith is acknowledged for review and proofreading.

References

Alpan, S., 1975. Geothermal energy exploration in Turkey. In: 2nd United Nation Symposium on the Development and Use of Geothermal Resources, San Francisco, CA, USA, p. 25.
Arnorsson, E., 1989. Deposition of calcium carbonate minerals from geothermal waters. Theoretical considerations. Geothermics 18, 33–39.
Baba, A., 2003. Geothermal Environmental Impact Assessment with Special Reference to the Tuzla, Geothermal Area, Canakkale Turkey. Geothermal Training Programme Book, Iceland, pp. 75–114.
Baba, A., Deniz, O., 2005. Determine of Potential, Application and Environmental Properties of Geothermal Resources in Biga Peninsula, TUBİTAK Project, ÇAYDAG-104Y082.
Baba, A., Özcan, H., 2004. Monitoring and evaluation of the geothermal fluid on soil and water in the Tuzla Geothermal Field by GIS. In: Erasmi, S., Cyffka, B., Kappas, M. (Eds.), Remote Sensing and GIS for Environmental Studies. Göttinger Geographische Abhandlungen, vol. 113, pp. 138–143.
Baba, A., Özcan, H., Deniz, O., 2005. Environmental impact by spill of geothermal fluids at the geothermal field of Tuzla, Canakkale-Turkey. In: Proceedings World Geothermal Congress 2005, Antalya, Turkey, 24–29 April 2005, pp. 1–8.
Baba, A., Yüce, G., Deniz, O., Uğurluoğlu, Y.D., 2009. Hydrochemical and isotopic composition of Tuzla Geothermal (Canakkale-Turkey) Field and its environmental impacts. J. Environ. Fresen. 10, 144–161.
Buckley, A.M., Greenblatt, M., 1994. The sol–gel precipitation of silica gels. J. Chem. Educ. 71, 599–602.
Demadis, K.D., 2010. Recent developments in controlling silica and magnesium silicate foulants in industrial water systems. In: Amjad, J. (Ed.), The Science and Technology of Industrial Water Treatment. IWA Publishing, London, New York, pp. 178–203.
Demir, M.M., Muñoz-Espí, R., Lieberwirth, I., Wegner, G., 2006. Precipitation of monodisperse ZnO nanocrystals via acid-catalyzed esterification of zinc acetate. J. Mater. Chem. 16, 2940–2947.
Demirörer, M., 1971. Resistivity Survey of Tuzla-Kestanbol Hot Springs and Surrounding, MTA report, Ankara (unpublished).
Drever, I., 1997. The Geochemistry of Natural Waters, Surface and Groundwater Environments, third ed. Prentice Hall, Upper Saddle River, NJ, pp. 164–178.
Ekingen, A., 1972. Gravimetric Survey of Ezine – Ayvacik – Bayramic Surrounding, MTA report, no.: 4859, Ankara.
Erdogan, E., 1966. Geothermal Energy Possibility of Survey and Tectonic Mapping of Tuzla Hot Springs and Surrounding, MTA report, Ankara (unpublished).
Gallup, D.L., 2002. Investigation on of organic inhibitors for silica scale control in geothermal brines. Geothermics 31, 415–430.
Garcia, Ad.V., Thomsen, K., Stenby, E.H., 2005. Prediction of mineral scale formation in geothermal and oilfield operations using the extended UNIQUAC model. Part I. Sulfate scaling minerals. Geothermics 34, 61–97.
Gevrek, A.I., Sener, M., 1985. The determination of hydrothermal alteration zones by clay minerals in Canakkale – Tuzla area. In: 2nd Turkish National Clay Symposium, Hacettepe University, Ankara, Turkey.
Gill, J.S., 1998. Silica scale control. Chem. Treatment, 41–45.
Gunnlaugsson, E., 1989. Magnesium-silicate scaling in mixture of geothermal water and deaerated fresh water in a district heating system. Geothermics 18, 113–120.
Honegger, J.L., Czernichowski-Lauriol, I., Criaud, A., Menjoz, A., Sainson, S., Guezennec, J., 1989. Detailed study of sulfide scaling at la courneuue nord, a geothermal exploitation of the Paris Basin, France. Geothermics 18, 137–144.
HU, 2008a. Evaluation Report on Geological, Hydrological Properties of T-7E ve T-8E Research/Production Well in Tuzla (Çanakkale) Geothermal Field, Ankara.
HU, 2008b. Evaluation Report on Geological, Hydrological Properties of T-10E Production Well in Tuzla (Çanakkale) Geothermal Field, Ankara.
Juranek, J., Skollova, Z., Harnova, J., 1987. MINEQUA—Part I. A program for computing the chemistry of calcium carbonate in mineralized and thermal waters. Geothermics 16, 263–270.
Karamanderesi, I.H., Öngür, T., 1974. The Report of Gradient Wells Tuzla (Canakkale) Geothermal Field. MTA report, no.: 5524, Ankara.
Keisuke, I., 1978. Ascending flow between the descending lithosphere and the overlying asthenosphere. J. Geophys. Res. 83, 262–268.
Kristmannsdóttir, H., 1989. Types of scaling occurring by geothermal utilization in Iceland. Geothermics 18, 183–190.
Lin, J.-K., Uan, J.-Y., Wu, C.-P., Huang, H.-H., 2011. Direct growth of oriented Mg–Fe layered double hydroxide (LDH) on pure Mg substrates and in vitro corrosion and cell adhesion testing of LDH-coated Mg samples. J. Mater. Chem. 21, 5011–5020.
MacDonald, G.J.F., 1956. Experimental determination of calcite–aragonite equilibrium relations at elevated temperatures and pressure. Am. Mineral. 41, 744–756.
Meyn, M., Beneke, K., Lagaly, G., 1990. Anion-exchange reactions of layered double hydroxides. Inorg. Chem. 29, 5201–5207.
MTA, 1997. 1/100 000 Scale-Geological Map, Biga Peninsula. General Directorate of Mineral Research and Exploration (MTA), Ankara.
Mutlu, H., Güleç, N., 1998. Hydrogeochemical outline of thermal waters and geothermometry applications in Anatolia (Turkey). J. Volcanol. Geotherm. Res. 85, 495–515.
Mützenberg, S., 1997. Nature and origin of the thermal springs in the Tuzla area, Western Anatolia, Turkey, Active Tectonic of Northwestern Anatolia – The Marmara Poly-Project. In: Schindler, C., Pfister, M. (Eds.), vdf hochschulverlag AG an der. ETH, Zurich, pp. 301–317.
Newton, R.C., Manning, C.E., 2000. Quartz solubility in H_2O-NaCl and H_2O-CO_2 solutions at deep crust-upper mantle pressures and temperatures: 2–15 kbar and 500–900 °C. Geochim. Cosmochim. Acta 64 (17), 2993–3005.
Ölçenoğlu, K., 1986. Scaling in the reservoir in Kizildere Geothermal Field, Turkey. Geothermics 15, 731–734.
Öngür, T., 1973. Volcanology and Geological Report of Canakkale Tuzla Geothermal Area, MTA Report, Ankara (unpublished).

Patzay, G., Karman, H.F., Pota, G., 2003. Preliminary investigations of scaling and corrosion in high enthalpy geothermal wells in Hungary. Geothermics 32, 627–638.
Pol, V.G., Gedanken, A., Calderon-Moreno, J., 2003. Deposition of gold nanoparticles on silica spheres. A sonochemical approach. Chem. Mater. 15, 1111–1118.
Potapov, V.V., Kashpura, V.N., Alekseev, V.I., 2001. A study of the growth of deposits in geothermal power systems. Therm. Eng. 48 (5), 395–400.
Şamilgil, E., 1966. Hydrogeological Report of Geothermal Energy Possibility Survey of Hot Springs of Kestanbol and Tuzla village of Canakkale. MTA report, no.: 4274, Ankara.
Şamilgil, E., 1983. Geothermal fields in Canakkale and Tuzla drills. Turkish Geol. Bull. 4, 147–148.
Şener, M., Gevrek, A., 2000. Distribution and significance of hydrothermal alteration minerals in the Tuzla hydrothermal system, Çanakkale, Turkey. J. Volcanol. Geotherm. Res. 96, 215–218.
Şimşek, S., Yıldırım, N., Gülgör, A., 2005. Developmental and environmental effects of the Kızıldere geothermal power project, Turkey. Geothermics 34, 234–251.
Ürgun, S., 1971. The geology of Tuzla – Kestanbol (Canakkale) Surrounding and Geothermal Energy Possibility, MTA report, no.: 4664, Ankara.
WES JEC, 2006. Report on Geothermal Development Survey in the Canakkale-Tuzla Field. West Japan Engineering Consultants, Inc., Turkey.
White, D.E., 1968. Environments and generations of some base metal ore deposits. Econ. Geol. 63 (4), 301–335.